

## The Influence of Si:Al and Na:Al On The Physical and Microstructure Characters of Geopolymers Based on Metakaolin

SUBAER<sup>1,a\*</sup>, ABDUL Haris<sup>1,b</sup>, NURHAYATI<sup>1,c</sup>, ANDI Irhamsyah<sup>1,d</sup>,  
JANUARTI Jaya Ekaputri<sup>2,e</sup>

<sup>1</sup>Laboratorium Fisika Material, Jurusan Fisika, Universitas Negeri Makassar, Indonesia  
Jl. Daeng Tata Raya, Makassar, Indonesia

<sup>2</sup>Department of Civil Engineering, Institut Teknologi Sepuluh Nopember, Sukolilo, Surabaya, 60111, Indonesia

<sup>a</sup>jzubayir@yahoo.com, <sup>b</sup>Abdulharis@yahoo.co.id, <sup>c</sup>Nurhayati\_unm@yahoo.com  
<sup>d</sup>irhamsyah.physics@gmail.com, <sup>e</sup>januarti\_je@yahoo.com

**Keywords:** geopolymers, metakaolin, physical properties, microstructure characters

**Abstract.** A research has been conducted to investigate the physico-mechanical and microstructure properties of geopolymers synthesised from metakaolin activated with sodium silicate solution. A wide range of physical and mechanical properties of geopolymers were studied such as bulk density, porosity, Vickers hardness, compressive strength, thermal expansion and thermal conductivity. It was found that these properties were directly related to geopolymers process variables such as Si:Al, Na:Al, Na<sub>2</sub>O:H<sub>2</sub>O, time and curing temperature. The structure of the resulting geopolymers was studied by using X-Ray diffraction (XRD) and the microstructure of geopolymers paste and the interfacial transition zone (ITZ) between the aggregate and the matrix of geopolymer were studied by using Transmission Electron Microscope (TEM) and Scanning Electron Microscope (SEM). The results gave a new insight into the composition-microstructure-property relationship of geopolymers and paving the way to the production of geopolymers with improved performance in a variety of applications.

### Introduction

Over the last thirty years, *geopolymers*, have received much attention as a promising new form of inorganic polymer material that could substantially substitute for conventional or ordinary Portland cement, plastics, ceramics-composites and many mineral-based products. Geopolymers are a subset of the broader class of alkali-activated binders [1]. The defining characteristic of a geopolymer is that the binding phase comprises an alkali aluminosilicate gel, with aluminium and silicon linked in a three-dimensional tetrahedral gel framework that is relatively resistant to dissolution in water [2,3].

Research has shown that geopolymers may be readily synthesised through alkali-activation of inexpensive and pure starting materials such as kaolinitic clays [4-10,26], as well as waste products such as fly ash and furnace slag [11-16].

Geopolymers have a potential for a wide variety of applications, whether used pure, with fillers or reinforced. In general, these applications can be divided into two categories; (1) Structural products such as reinforced for the manufacture of moulds, tooling, cement and concrete replacements in various environments, (2) Immobilisation technology for toxic chemical and radioactive waste containment. It is expected that in the near future these applications will also be found in automobile and aerospace industries, non-ferrous foundries and metallurgy, civil engineering and plastic industries [18-21]. Understanding of geopolymers is built to the point where binder properties can be tailored a priori by rational mix design, and the understanding of the binder structure is sufficient to explain why these properties can be expected to last for a sufficient period of time to render the material fit for purpose in an engineering sense [22].

## Experimental

Geopolymers produced in this study were prepared by the alkali-activation (sodium silicate solution) of metakaolin. Metakaolin was obtained by dehydroxylation of kaolinite at 750°C for 6 hours. Chemical compositions of the activation solution in terms of the molar oxide ratio used in this study were divided into 3 groups. In each group, the nominal Si:Al ranged from 1 to 2 while varying Na:Al from 0.6 for group A, 0.8 for group B and 1.0 for group C. The oxide molar ratio of H<sub>2</sub>O:Na<sub>2</sub>O was kept at a value of 10. The resulting geopolymer resin was poured into the moulds, compacted and vibrated few minutes and allowed to mature at room temperature for 30 - 60 minutes. Curing was undertaken at 70 °C for 2 hours followed by drying at room temperature before demoulding. Natural sand ( $\alpha$ -quartz) was used as aggregate and poured directly into the geopolymer resin. The grain size and concentration of sand aggregate used were 40  $\mu$ m, 125  $\mu$ m, 212  $\mu$ m, 500  $\mu$ m and 750  $\mu$ m, and 10 wt %, 20 wt %, 30wt % and 50 wt %, respectively. Another type of aggregate used was granite (known as blue metal), which was crushed and sieved to attain a grain size of 300  $\mu$ m and 600  $\mu$ m.

The resulting materials were subjected to various physico-mechanical characterisations, including bulk density, apparent porosity, vickers microhardness, compressive strength, aggregate-geopolymers interfacial bond, thermal conductivity, and thermal expansion. The structure of geopolymers was studied by using X-Ray diffraction (XRD). The microstructure of geopolymers paste and the interfacial transition zone (ITZ) between the aggregate and the matrix were studied by using Transmission Electron Microscope (TEM) and Scanning Electron Microscope (SEM).

## Results and Discussion

Fig. 1 depicted the XRD of metakaolin indicates all the kaolinite reflections have been eliminated leaving an amorphous pattern with ancillary peaks due to  $\alpha$ -quartz (SiO<sub>2</sub>) and anatase (TiO<sub>2</sub>) although the morphology of the original kaolinite is maintained as depicted in fig. 1.

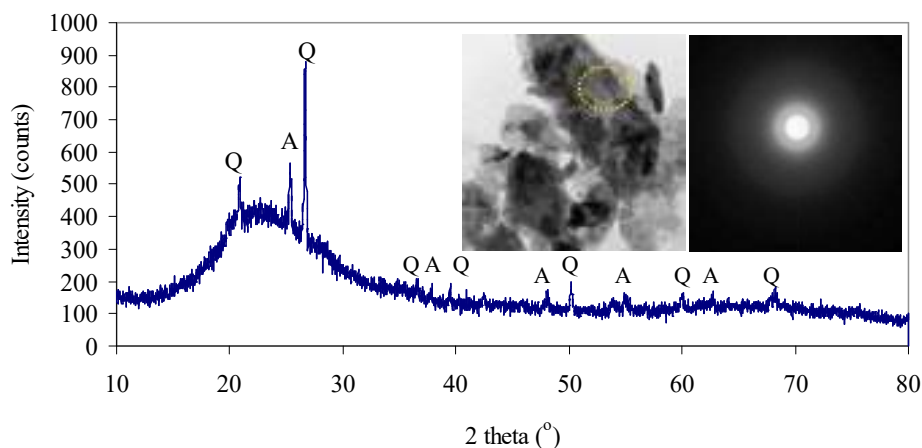


Figure 1. XRD pattern of metakaolin, A = anatase (TiO<sub>2</sub>) and Q =  $\alpha$ -quartz (SiO<sub>2</sub>), decorated with its TEM image and Selected Area of Electron Diffraction (SAED).

Geopolymers prepared in this study were divided into three groups based on the nominal ratio of atomic Si:Al and Na:Al. Geopolymers with Si:Al = 1.04 and 1.25 are designated as *sodium-poly(sialate)* (Na-PS) type, and geopolymers with Si:Al = 1.50, 1.75 and 2.00 are designated as *sodium-poly(sialate-siloxo)* (Na-PSS) type. The bulk density and apparent porosity of all specimens were measured by using Archimedes method. It was found that magnitude of the bulk density range from 1.40 to 1.70 g/cm<sup>3</sup> and the apparent porosity from range from 33 to 24%. Both parameters depend on the ratio of Si:Al and Na:Al.

The XRD results showed that all Na-PS type geopolymers enclose the formation of zeolite-A and zeolite-X (Fig. 2a). These material revealed low bulk density, high porosity, and low compressive

strength. The formation of zeolite-A and zeolite-X from the geopolymer processing route was also observed by Rowles & O'Connor [23]. They also reported that the formation of zeolite from the geopolymer route occurs with either low Si:Al or high Na:Al ratios. Similarly, Grutzeck, Kwan & DiCola [25] reported the formation of zeolite in alkali-activated cement based on fly-ash. Na-PSS geopolymers were formed by increasing the Si:Al atomic ratio from 1.50, 1.75 and 2.00 for Na:Al atomic ratios of 0.6, 0.8 and 1.0. For these compositions the XRD patterns indicated that the structure of the resulting geopolymers were essentially amorphous. Fig. 2 (b) shows the XRD patterns of a series of Na-PSS geopolymers formed with a Na:Al atomic ratio = 0.6.

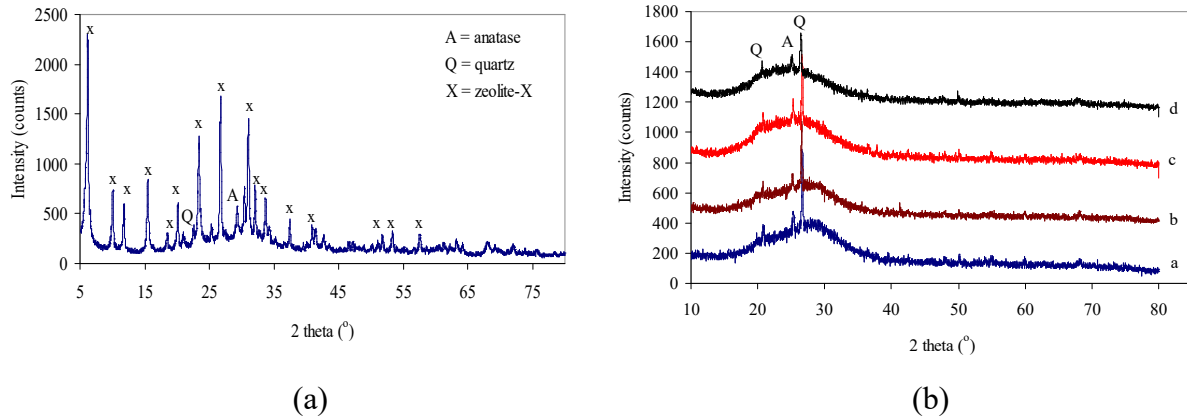


Figure 2. XRD patterns of geopolymers prepared with Na:Al molar ratio of 0.6. (a) Si:Al = 1.25, (b) Si:Al = 1.50, (c) Si:Al = 1.75 and (d) Si:Al = 2.0. The sharp diffraction peaks are anatase (A) and quartz (Q). Each pattern has been offset for clarity.

The diffraction patterns of these geopolymers, like the pattern of the original metakaolin, have a broad amorphous hump in the region  $20^\circ - 38^\circ(2\theta)$ . This suggests that the Na-PSS geopolymers consist of disordered frameworks with short-range order, with structures similar to those of felspathic glasses [23,8].

Fig. 3(a) show SEM images of a sample prepared with Si:Al = 1.25 and Na:Al = 0.8. Based on the XRD results, a greater amount of zeolite-A was formed in this sample. Fig. 3(b) shows SEM image of a sample with Si:Al = 1.25, Na:Al = 1.0. The sample appears more dense than the sample shown in fig. 2 (a). Large voids on the surface of the sample are believed to be due to the grain pullout during polishing. The images indicates the influence of composition (Na:Al) to the microstructure characters of geopolymers.

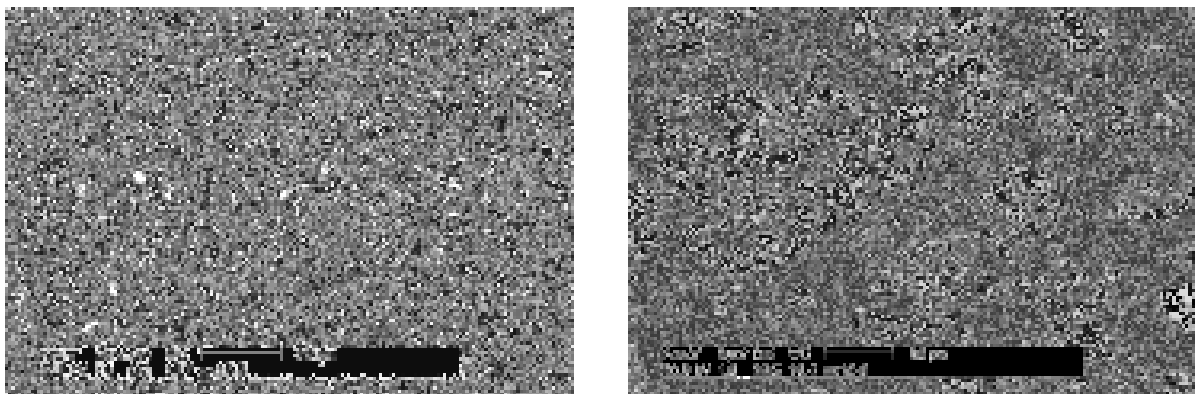


Figure 3. (a) SEM image of a geopolymer sample with Si:Al = 1.25, Na:Al = 0.8, (b) SEM image of geopolymer sample with Si:Al = 1.25, Na:Al = 1.0.

Fig. 4(a) shows that geopolymer prepared with Si:Al = 2.0, Na:Al = 1.0 has high homogeneity. This indicates that there was adequate sodium silicate solution to be able to dissolve most of the

metakaolinite resulting in hardened geopolymer paste after curing. The presence of unreacted metakaolin was further investigated by using TEM (fig. 4b). Selected area electron diffraction (SAED) examination on these sites revealed no sign of crystallinity.

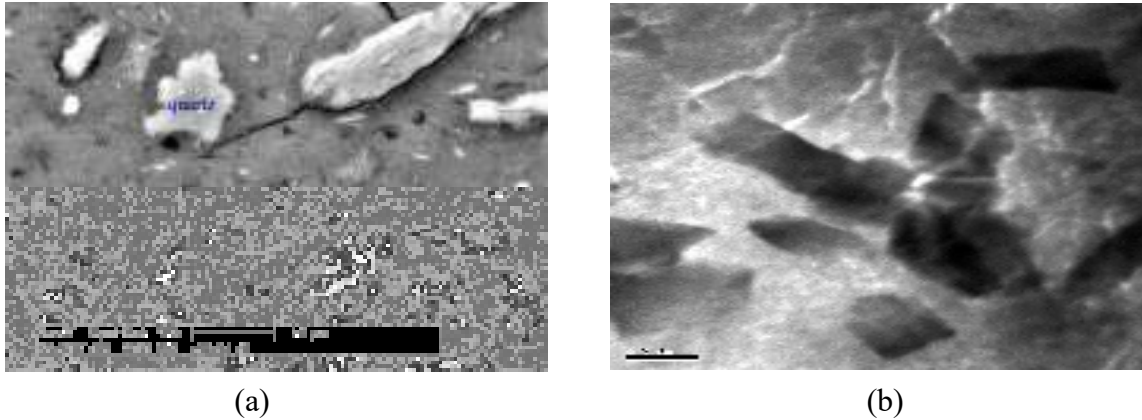


Figure 4. (a) SEM image of geopolymer sample with Si:Al = 2.0, Na:Al = 1.0 showing high homogeneity of the geopolymer matrix, (b) A representative TEM image for a geopolymer sample with Si:Al = 2.0, Na:Al = 1.0 showing unreacted metakaolinite (dark grains) surrounded by geopolymer matrix.

The thermal expansion and shrinkage behaviour of geopolymers measured using a DI-24 Adamel Limohargy dilatometer. Fig. 5(a) shows the dilatometer curve of an as prepared geopolymer with Si:Al = 1.50, Na:Al = 0.6 measured from about 23 °C to 900 °C with a heating rate of 2 °C/minute.

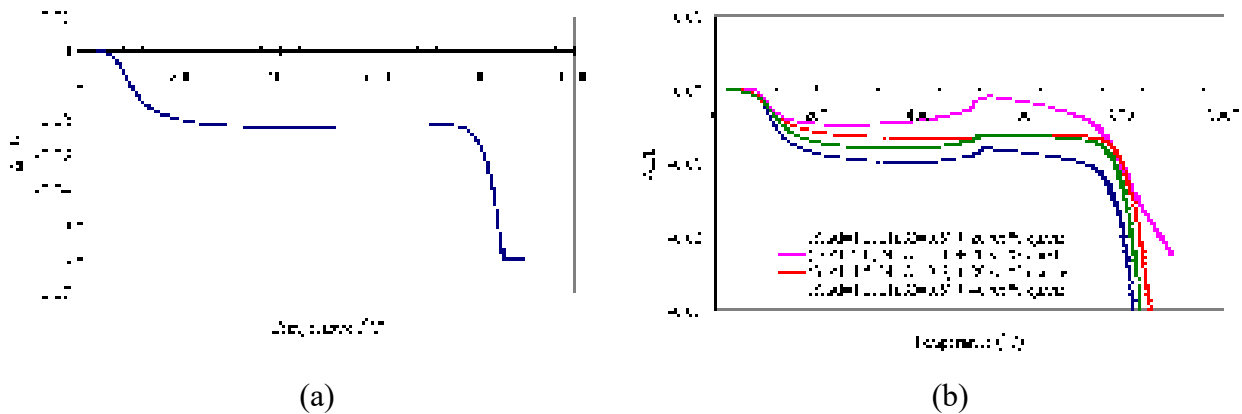


Figure 5. (a) Dilatometer curve for geopolymer with Si:Al = 1.5, Na:Al = 0.6.  $\Delta L$  is the change in length, (b) Dilatometer curves for geopolymers containing quartz and granite aggregate.

The curve show that the water loss (about 15 wt %) from room temperature up to 250 °C is associated with about 2 % shrinkage. Between 250 and 800 °C the geopolymer is essentially dimensionally stable indicating that this may be a useful working temperature range. Further substantial shrinkage from about 800 °C to 900 °C occurs due to densification within the sample bulk and was beyond the range of the dilatometer. The shrinkage behaviour of geopolymer reported in this study is in good agreement with the results reported by Barbosa & MacKenzie [26]. The calculation of coefficient thermal expansion ( $\alpha_T$ ) versus temperature for geopolymer with Si:Al = 1.5, Na:Al = 0.6 shows that the coefficient of thermal expansion of geopolymer is negative and increases rapidly from 100 °C ( $\alpha = -0.2 \times 10^{-5} \text{ } ^\circ\text{C}^{-1}$ ) to 250 °C ( $\alpha = 7.6 \times 10^{-5} \text{ } ^\circ\text{C}^{-1}$ ) and gradually decreases from 300 °C to 750 °C ( $\alpha = -5.2 \times 10^{-5} \text{ } ^\circ\text{C}^{-1}$ ).

Fig. 5 shows dilatometer curves for geopolymers containing quartz and granite aggregate. The presence of aggregates (20 wt %) was found to significantly reduce the shrinkage to about 1 % in the

temperature range between 23 and 500 °C. A higher content of quartz aggregate (40 wt %) was found to further reduce the shrinkage. The effect of quartz aggregate on reducing the shrinkage is very significant for geopolymer prepared with Si:Al = 2.0, Na:Al = 1.0, albeit with severe cracking.

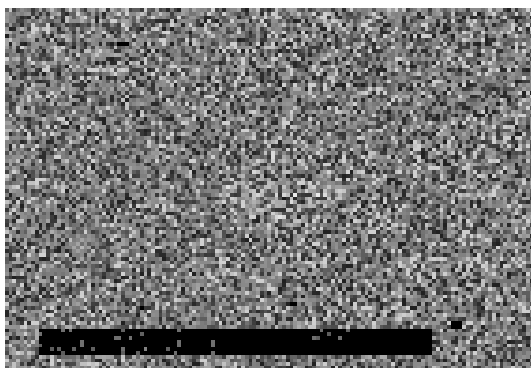
Fig. 5 indicates that although the inclusion of quartz has a significant effect in reducing the shrinkage of geopolymers at elevated temperatures, the useful upper working temperature is restricted 500 °C. For this reason, fire-resistant concrete based on Portland cement is never made with quartz aggregate [27].

Geopolymers have been recognised as a potential substitute material for ordinary Portland cement as well as being suitable for insulation purposes and hence its thermal conductivity is important property. The technique employed to measure the thermal conductivity of geopolymers in this study was a hot-wire method. Table 1 shows the value thermal conductivity of geopolymers measured in this study. The values of the thermal conductivity of the sample TC-03 (Si:Al = 2.0; Na:Al = 1.0) is slightly lower than that of TC-01 (Si:Al = 1.5, Na:Al = 0.6) and TC-02 (Si:Al = 1.5, Na:Al = 0.8). The difference in thermal conductivity for these samples is believed due to the differences in their bulk density.

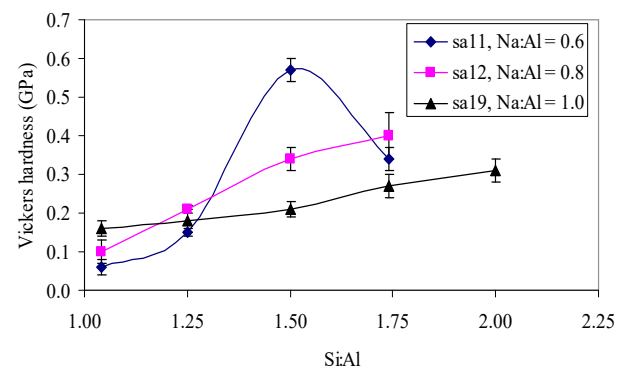
Table 1. Density and thermal conductivity of geopolymers.

Sample ID	Density (g cm <sup>-3</sup> )	Thermal conductivity (W m <sup>-1</sup> K <sup>-1</sup> )
TC-01 (Si:Al = 1.5, Na:Al = 0.6)	1.68 (0.09)	0.65 (0.04)
TC-02 (Si:Al = 1.5, Na:Al = 0.8)	1.62 (0.05)	0.64 (0.03)
TC-03 (Si:Al = 2.0, Na:Al = 1.0)	1.43 (0.01)	0.55 (0.03)

Vickers hardness tests were performed to measure the geopolymers' resistance to plastic deformation. As a cementitious type of material, geopolymers do not have a very high hardness and therefore the applied load should be in the range 0.1 to 1.5 kg, referred to as low load hardness. Fig. 6 (a) shows the indent of geopolymer Si:Al = 1.5 and Na:Al = 0.6 which has the highest hardness and (b) shows the value of Vickers hardness as a function of Si:Al. The hardness of all specimens increases in an almost linear fashion as the Si:Al increases except for the sample with Si:Al = 1.50, Na:Al = 0.6.



(a)



(b)

Figure 6. (a) SEM micrograph of Vickers indentation of Si:Al = 1.5, Na:Al = 0.6 (load = 1 kg), (b) Vickers hardness as a function of Si:Al for three different values of Na:Al. Error bars represent 2SD.

Fig. 7 (a) is a plot of compressive strength as a function of Si:Al for three different series of samples measured after ageing the samples between 7 to 14 days. A Si:Al ratio of 1.5 (Na:Al = 0.6) was found to produce the highest compressive strength ( $86 \pm 16$  MPa). It is notable that for samples with a Na:Al = 1.0, the maximum strength occurred at Si:Al = 1.75 and Si:Al = 2.0. Fig. 7(b) shows

the relationship between the porosity and the compressive strength of the samples shown in fig. 7(a). As expected, the strength of the material decreases as the porosity increases.

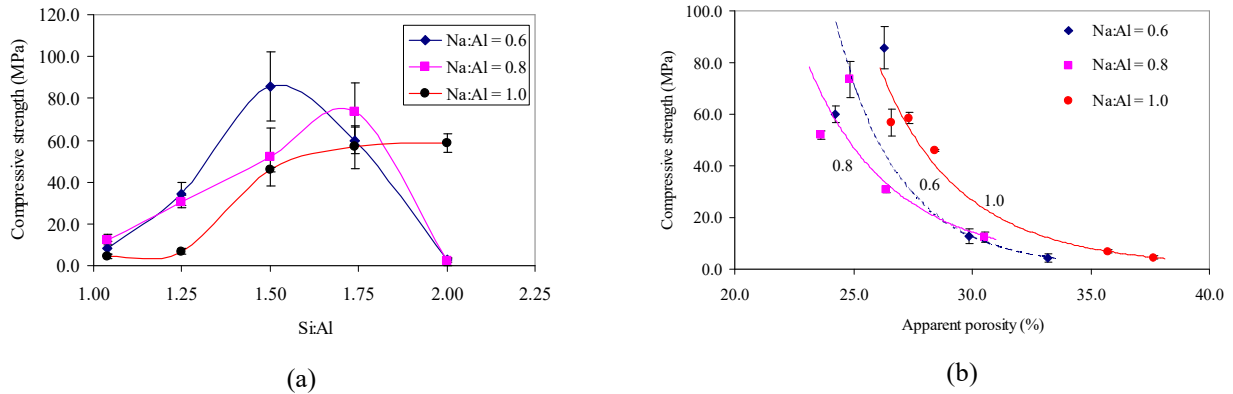


Figure 7. (a) Compressive strength of geopolymers prepared with different initial ratios of Si:Al and Na:Al. (b). Compressive strength as a function of apparent porosity for different Si:Al ratios. Error bars represent 2SD.

The incorporation of aggregate into the geopolymers paste was aimed particularly at increasing the strength of the resulting materials through the densification of the matrix. Fig. 8 shows compressive strength as a function of aggregate (quartz) content. The curve shows a sharp decrease in compressive strength for aggregate content greater than 40 wt%. This is believed to be due in part to the fact that as the amount of aggregate increases the workability of the mixture decreases preventing thorough mixing which may lead to reduce the bond strength between aggregate and geopolymer paste (Fig. 8b). Also as the aggregate content increases the amount of geopolymer available to deflect and absorb cracks decreases which ultimately limits the strength of the material. Similar result was reported by Hos, McCormick & Byrne [28].

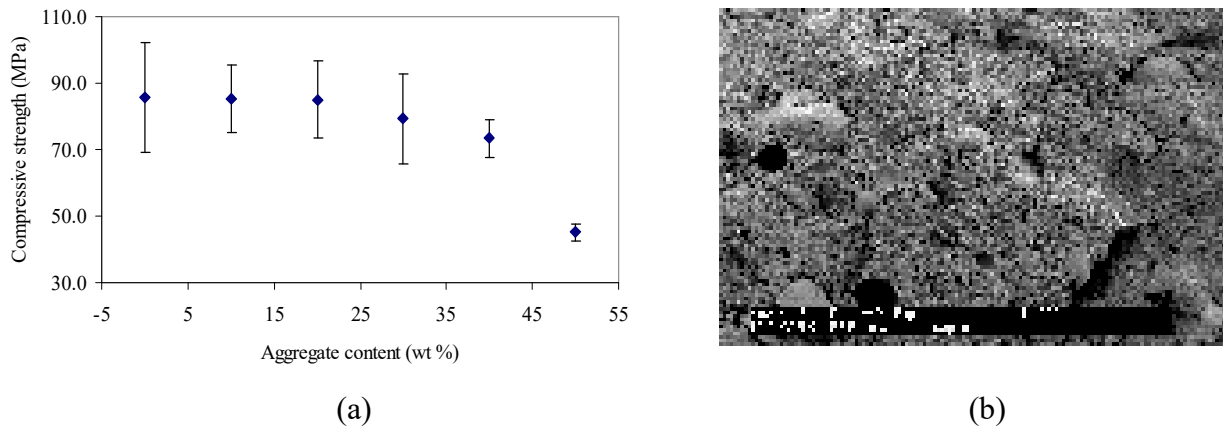


Figure 8. (a) Compressive strength as a function of quartz aggregate (< 212  $\mu\text{m}$ ) content (Si:Al = 1.50, Na:Al = 0.6). Error bars represent 2 SD. (b) SEM image of a fractured geopolymer specimen (Si:Al = 1.5; Na:Al = 0.6) containing quartz aggregate. No broken quartz was observed.

## Summary

- Geopolymers based on metakaolin synthesised were divided into two groups; *sodium-poly(sialate)* (Na-PS) (Si:Al = 1.04 and 1.25) and *sodium-poly(sialate-siloxo)* (Na-PSS) (Si:Al = 1.50, 1.75 and 2.00) geopolymers.
- The XRD patterns revealed that Na-PS geopolymer consists of zeolite-A or zeolite-X in conjunction with amorphous aluminosilicate, while Na-PSS geopolymers were amorphous with a broad hump in the region  $20^\circ - 38^\circ$  ( $2\theta$ ).

- Si:Al and Na:Al ratio of the starting materials play important roles in determining the mix design as well as the ultimate physical and microstructure characters of the resulting geopolymers and intended applications.

## References

- [1] Shi C., Krivenko P.V. and Roy D. (2006), *Alkali-activated Cements and Concretes*, Taylor & Francis, London.
- [2] Mackenzie, K. J. D. (2003) What are these things called geopolymers? A physico-chemical perspective. *Ceramic Transactions*, 153, 175–186.
- [3] Rees, C. a., Provis, J. L., Lukey, G. C. and van Deventer, J. s. J. (2007) attenuated total reflectance Fourier transform infrared analysis of fly ash geopolymer gel ageing. *Langmuir*, 23, 8170–8179.
- [4] Davidovits, J. (1982), "Mineral polymers and methods of making them", 4,349,386 United States Patent.
- [5] Rahier, H., Van Melle, B., Biesemans, M., Wastiels, J. & Wu, X. (1996), "Low-temperature synthesized aluminosilicate glasses Part I Low-temperature reaction stoichiometry and structure of a model compound", *Journal of Materials Science*, 31, 71-79.
- [6] Rahier, H., Simons, W., Van Melle, B. & Biesemans, M. (1997), "Low-temperature synthesized aluminosilicate glasses Part III *Influence of composition of the silica solution on production, structure and properties*", *Journal of Materials Science*, 32, 2237-2247.
- [7] Granizo, M. L., Blanco-Varela, M. T. & Palomo, A. (2000), "Influence of the starting kaolin on alkali-activated materials based on metakaolin. Study of the reaction parameters by isothermal conduction calorimetry", *Journal of Materials Science*, 35, 6309-6315.
- [8] Barbosa, V. F. F., MacKenzie, K. J. D. & Thaumaturgo, C. (2000), "Synthesis and characterisation of materials based on inorganic polymers of alumina and silica: sodium polysialate polymers", *International Journal of Inorganic Materials*, 2, (4), 309-317.
- [9] Subaer and Van Riessen, A. (2007) Thermo-mechanical and microstructural characterisation of sodium-poly(sialate-siloxo) (Na-PSS) geopolymers. *Journal of Materials Science*, 42, 3117–3123.
- [10] Ekaputri, J.J., Triwulan, Subaer, J., Fansuri, H., and Aji, R.B., "Light Weight Geopolymer Paste made with Sidoarjo Mud (Lusi) ", *Materials Science Forum* Vol. 803 (2015) pp 63-74
- [11] Jiang, L. & Guan, Y. (1999), "Pore structure and its effect on strength of high-volume fly ash paste", *Cement and Concrete Research*, 29, 631-633.
- [12] Palomo, A., Grutzeck, M. W. & Blanco, M. T. (1999), "Alkali-activated fly ashes A cement for the future", *Cement and Concrete Research*, 29, 1323-1329.
- [13] van Jaarsveld, J. G. S., van Deventer, J. S. J. & Lorenzen, L. (1997), "The potential use of geopolymeric materials to immobilise toxic metals: Part I. Theory and applications", *Minerals Engineering*, 10, (7), 659-669.
- [14] van Jaarsveld, J. G. S. & van Deventer, J. S. J. (1999), "The effect of metal contaminants on the formation and properties of waste-based geopolymers", *Cement and Concrete Research*, 29, 1189-1200.
- [15] Brough, A. R. & Atkinson, A. (2002), "Sodium silicate-based, alkali-activated slag mortars Part I. Strength, hydration and microstructure", *Cement and Concrete Research*, 32, 1 - 15.

- 
- [16] Swanepoel, J. C. & Strydom, C. A. (2002), "Utilisation of fly ash in a geopolymeric material", *Applied Geochemistry*, 17, (8), 1143 - 1148.
- [17] Cheng, T. W. & Chiu, J. P. (2003), "Fire-resistant geopolymer produced by granulated blast furnace slag", *Minerals Engineering*, 16, 205 - 210.
- [18] Hardjito, D., Wallah, S. E., Sumajouw, D. M. J. and Rangan, B. V. (2004) On the development
- [19] of fly ash-based geopolymer concrete. *ACI Materials Journal*, 101, 467–472.
- [20] Xu, H. & van Deventer, J. S. J. (2000), "The geopolymerisation of alumino-silicate minerals", *International Journal of Mineral Processing*, 59, 247-266.
- [21] Lyon, R. E., Balaguru, P. N., Foden, A., Sorathia, U., Davidovits, J. & Davidovics, M. (1997), "Fire resistant aluminosilicate composites", *Fire and Materials*, 21, 67-73.
- [22] Provis, J.L., and van Deventer, J.S.J "Geopolymers Structure, processing, properties and industrial applications", 2009, Woodhead publishing limited, Oxford.
- [23] Rowles, M. & O'Connor, B. H. (2003), "Chemical optimisation of the compressive strength of aluminosilicate geopolymers synthesised by sodium silicate activation of metakaolinite", *Journal of materials chemistry*, 13, (13), 1-6.
- [24] Grutzeck, M., Kwan, S. & DiCola, M. (2004), "Zeolite formation in alkali-activated cementitious systems", *Cement & Concrete Research*, 32, 949-955.
- [25] Davidovits, J. (1991), "Geopolymers: Inorganic Polymeric New Materials", *Journal of Thermal Analysis*, 37, 1633-1656.
- [26] Barbosa, V. F. F. & MacKenzie, K. J. D. (2003), "Thermal behaviour of inorganic geopolymers and composites derived from sodium polysialate", *Materials Research Bulletin*, 38, (2), 319 - 331.
- [27] Neville, A. M. (2000) *Properties of concrete*, Prentice Hall, Harlow.
- [28] Hos, J. P., McCormick, P. G. & Byrne, L. T. (2002), "Investigation of a synthetic aluminosilicate inorganic polymer", *Journal of Materials Science*, 37, 2311-2316.